

# EFFECT OF PRE-QUENCHING PROCESS ON MICROSTRUCTURE AND MECHANICAL PROPERTIES OF ULTRA-HIGH STRENGTH DUAL PHASE STEEL \*

Jiayu Li <sup>1</sup>  
Yunbo Xu <sup>2</sup>  
Jianping Li <sup>3</sup>  
Fei Peng <sup>4</sup>  
Yu Wang <sup>5</sup>  
Xingli Gu <sup>6</sup>  
Hua Zhan <sup>7</sup>

## Abstract

In this study, in order to achieve ultra-high strength without reducing plasticity, a novel heat treatment involving a pre-quenching process prior to conventional intercritical annealing (P-IDP) was proposed in a low carbon low alloy DP steel. It revealed that abundant fraction of banded structure was observed after conventional intercritical heat treatment (IDP) due to the inheritance of cold rolling deformation. However, the banded structure in novel heat treatment was eliminated significantly, whilst the refined microstructure was relatively more homogeneous with ultrafine ferrite grains. Moreover, obvious chain-networked martensite grains along the ferrite grain boundaries were obtained. The optimum mechanical properties with ultimate strength of 1238 MPa, total elongation of 17%, product of strength and elongation (PSE) of 21GPa% were obtained by P-IDP treatment, which was much higher than the values reported with similar composition. As to pre-quenching treatment, all of grain refinement, homogeneous distribution of martensite islands and precipitated strengthening of microalloyed carbides were beneficial to improve the final strength and ductility.

**Keywords:** Dual phase steel ; Pre-quenching process ; Ultra-high strength ; Ductility.

<sup>1</sup> *PhD Candidate, The State Key Laboratory of Rolling and Automation, Northeastern University, Shenyang, China.*

<sup>2</sup> *Professor, The State Key Laboratory of Rolling and Automation, Northeastern University, Shenyang, China.*

<sup>3</sup> *Professor, The State Key Laboratory of Rolling and Automation, Northeastern University, Shenyang, China.*

<sup>4</sup> *PhD Candidate, The State Key Laboratory of Rolling and Automation, Northeastern University, Shenyang, China.*

<sup>5</sup> *PhD Candidate, The State Key Laboratory of Rolling and Automation, Northeastern University, Shenyang, China.*

<sup>6</sup> *PhD Candidate, The State Key Laboratory of Rolling and Automation, Northeastern University, Shenyang, China.*

<sup>7</sup> *Chief Engineer, Maanshan Iron & Steel Company Limited, Maanshan, China.*

## 1 INTRODUCTION

As an effective way to reduce fuel consumption and emission, the application of advanced high strength steel (AHSS) can effectively achieve lightweight of automobile. As a representative one of AHSS, dual phase (DP) steel that mainly composed of martensite and ferrite possesses excellent mechanical properties, good formability and low cost, which lead to the wide application of DP steel in the automotive industry [1-4]. Generally, DP steel is obtained by thermo-mechanical rolling process [5,6] or annealing at the two-phase intercritical region followed by rapid cooling [7,8].

In recent years, the development of AHSS is focused on the improvement of both strength and elongation. As one of most widely commercial AHSS [9], DP steel has been paid a great attention to develop the ultra-high strength with good ductility. Many strengthening mechanisms were applied to improve the strength of DP steel. In particular, micro-alloyed elements, such as Nb, V, and Ti, Mo, are usually used to improve strength of DP steel. Fruitful studies have been carried out about the effect of microalloyed elements on the improvement of mechanical properties. Song et al. [10] investigated DP steel with four levels of Nb content (0, 0.021, 0.038 and 0.063 wt%), indicating that the increase in Nb addition can significantly increase the yield strength and tensile strength of DP steels. Chen et al. [11] studied the mechanical properties of DP steels with additions of Ti, Ti-Mo and Ti-Nb elements, respectively. The result emphasizes that (Ti,Mo)C particles have a vital contribution to the strength of the steel. Hong et al. [12] reported that Nb and V additions could prevent grain growth in hot rolled DP steels. Papa Rao et al. [13] investigated the V-Nb precipitates in UFG DP steel. It was shown that the nanoscale VC and NbC improved the strength and work hardening exponent of UFG DP steel. Furthermore, grain refinement is also an

effective way to strengthening DP steel. Hashemi et al. [14] conducted three steps to achieve ultrafine grained DP steel and obtained appropriate combination of strength and elongation. Calcagnotto et al. [15], has applied a large-strain warm deformation to obtain UFG microstructure. Sun et al. [16] used an warm rolling intercritical annealing to produce a lamellar-structured (UFG) DP steel.

However, the strengthening methods of DP steel by adding alloying elements and/or complex processing are not suitable for industrial production. Actually, both of them increase the cost and improve the difficulty of wide production. The key to solve this problem is to develop an industrially feasible way to improve the mechanical properties without dramatically increasing cost and deteriorating formability.

Therefore, in this article, a novel pre-quenching process was applied to a low carbon low alloy DP steel. The objective is to elucidate the influence of pre-quenching process on microstructural evolution and mechanical properties in DP steel. All of the microstructure characteristics, phase transformation behavior and final mechanical properties were compared between pre-quenching DP steel and traditional DP steel, which were obtained based on the results of microstructure characterization and dilatometric analysis. The microstructures were characterized using scanning electron microscopy (SEM), electron backscatter diffraction (EBSD) and transmission electron microscopy (TEM).

## 2 MATERIAL AND METHODS

A low carbon low alloy DP steel was investigated in the present study and the chemical composition is listed in Table 1. A 70kg ingot was homogenized at 1250°C for 2.5h, and hot rolled to 3.2mm thickness with a finish-rolling temperature of 890°C. Then the plate was annealed at 680°C for 1h, followed by furnace cooling to ambient temperature. Subsequently, the plate was

cold-rolled to about 1.2mm after pickling in 10 vol% hydrochloric acid. The tensile specimens for heat treatment were machined from the cold-rolled sheet along the rolling direction with gage length of 50mm and width of 12.5mm.

In order to understand the phase transformation behavior of experimental steel and establish appropriate heat treatment schedule, the dilatometry experiment were carried out by using the DIL 805 A/D dilatometry. The dilatometric samples with dimensions of 10mm × 4mm × 1.2mm were prepared from cold rolled sheets. The sample was heated at 10°C /s from room temperature to 900°C, held for 300s, and then quenched to room temperature with a cooling rate of 40°C /s. The critical temperature of Ac1, Ac3, Ms and Mf can be determined on basis of the dilatometric result in Fig. 1 as 735°C, 850°C, 400°C and 230°C, respectively. It is worth noting that no other phase transformation occurred during the cooling process, until below the Ms temperature.

**Table 1.** Chemical compositions of the experimental steel (wt%).

C	Mn	Cr	Mo	Nb+Ti+V
0.07	2.3	0.39	0.28	<0.1

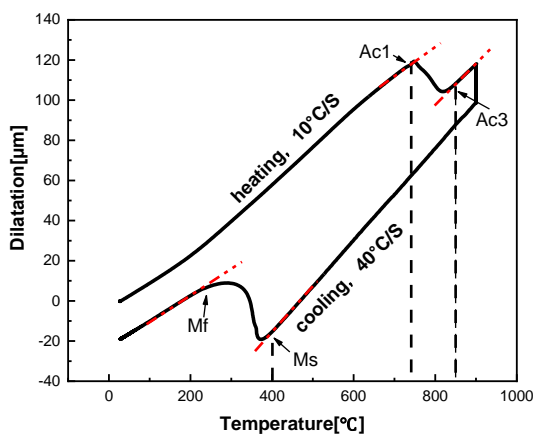


**Figure 1.** Dilatometric results of intercritical temperatures (Ac1, Ac3, Ms and Mf) for the experimental steel.

The heat treatments of tensile specimens presented in Fig.2 were carried out in a tube resistance furnace and salt baths. Here two series of heat treatments were

conducted, one is conventional intercritical heat treatment process of DP steel (IDP), and the other is involved a pre-quenching process followed by intercritical heat treatment (hereafter referred to as P-IDP). The IDP specimens were annealed at different intercritical temperatures for 300s, including 740°C, 760°C, 780°C, 800°C, 820°C. Subsequently, all samples were overaged at 460°C for 30s in salt bath furnace, followed by air quenching to room temperature. In contrast, the P-IDP specimens were firstly annealed at 900°C for 300s to full austenitization, followed by fast quenching to room temperature by water to obtain full martensite structure. Subsequently, an intercritical annealing process with identical conditions of IDP was applied.

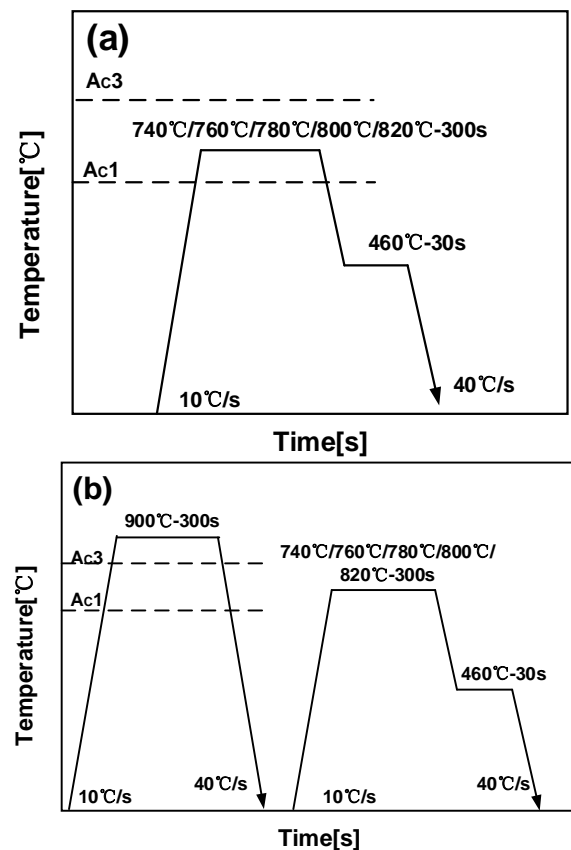


**Figure 2.** Schematic diagrams of different heat treatments.(a) IDP; (b) P-IDP

The mechanical properties of tensile specimens were measured on an INSTRON 10 kN machine at room temperature with a strain rate of 3mm/min. The corresponding microstructures were

characterized by ZEISS ULTRA 55 field emission scanning electron microscopy (SEM). In order to analysis the element distribution, map scanning was performed using JEOL JXA-8530F electron probe microanalyzer (EPMA). The analysis of Electron backscattered diffraction (EBSD) was applied to samples with 20kV and a step size of 0.05 $\mu$ m. All samples for EBSD were prepared by electro-chemical polishing, and parameters are 12V for 20s. The specimens were applied for microstructure observation using a FEI G2 F20 transmission electron microscope (TEM) with operation voltage of 200 KV.

### 3 RESULTS AND DISCUSSION

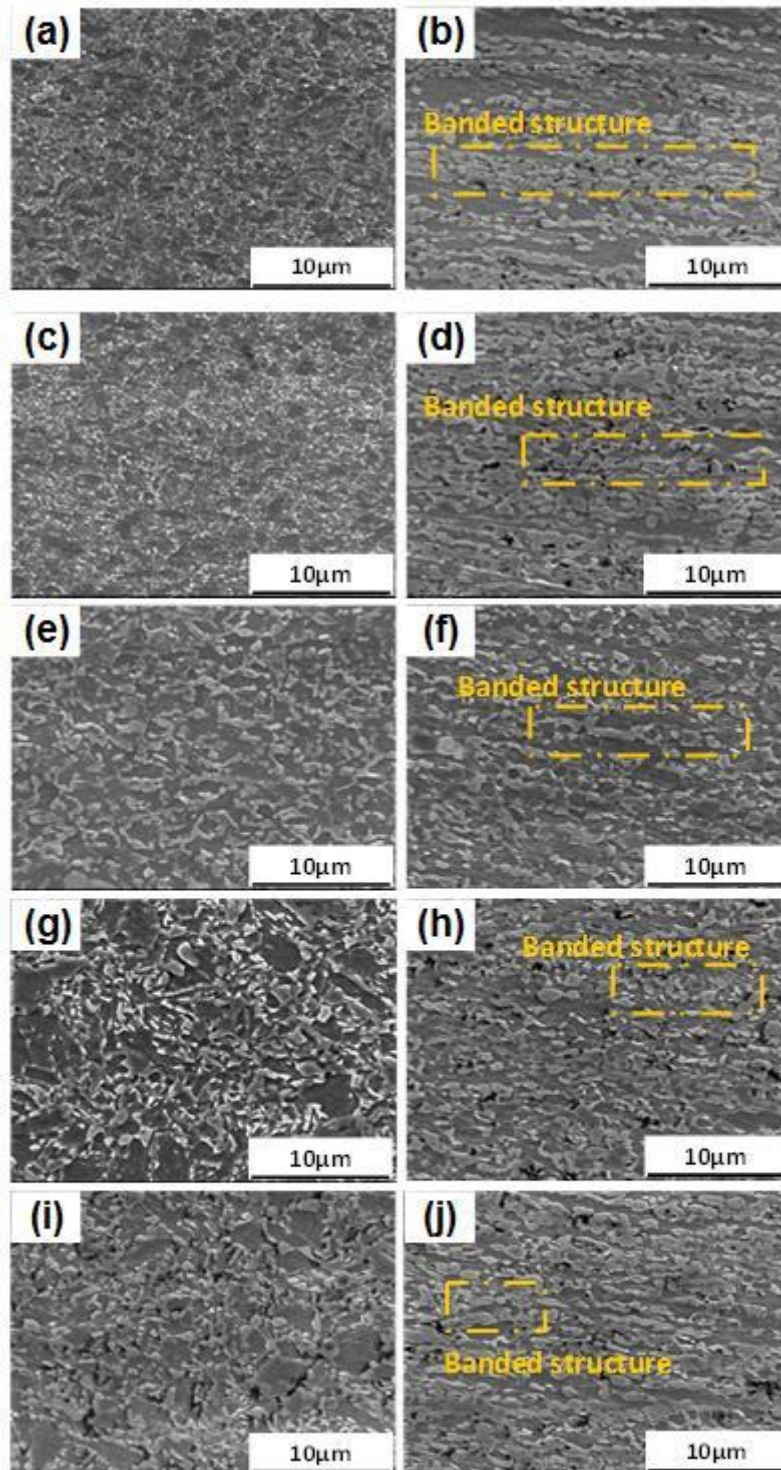
#### 3.1 Effect of pre-quenching process on microstructure evolution

Fig.3 shows SEM micrographs of IDP and P-IDP samples. It is clear that the microstructure of IDP sample is composed of ferrite (F) and martensite (M), which is typical microstructure in DP steel. Meanwhile, the banded structure was significantly observed in all samples, while gradually decreased with increasing annealing temperature. Actually, the banded structure was usually reported as a result of element segregation, especially Mn element, or an inheritance of cold rolling structure [17,18]. As to the P-IDP samples, it can be found that the microstructure at low annealing temperature (Fig. 3a and 3c), is composed of tempered martensite, whilst abundant fraction of undissolved cementite is observed. Hence, it can be deduced that the start structure of quenched martensite can retard the subsequent austenitization

process. Moreover, as increasing annealing temperature to 780°C and above, the austenite was formed during annealing process, whilst the prior martensite tempered and recrystallized in a low temperature regime [19]. It is worthwhile to note that there was no existence of banded structure in all P-IDP samples, which means that the pre-quenching treatment can significantly eliminate banded structure. As compared with IDP samples, the microstructure of P-IDP samples was dramatically refined, which is composed of ultra-fine martensite island with size of less than 2  $\mu$ m and ferrite with homogeneous distribution. Overall, the martensite volume fraction of IDP and P-IDP samples both increased with increasing annealing temperature.

As to the case of IDP samples, the start structure consists of deformed ferrite and deformed pearlite, which were both elongated after cold rolling. During the intercritical annealing process, the austenite was preferentially nucleated at the interface of cementite and ferrite. As the carbon diffusion between cementite and austenite was much faster than that between ferrite and austenite. Hence, the austenite grew into cementite quickly to inherit the lath-like morphology of cementite. Finally, the lath-like austenite transformed into martensite island, which is the band structure observed in Fig. 3.

However, as to the P-IDP process, the cold-rolled structure was fully austenitized during the pre-quenching process. Subsequently, the austenite nucleated at the interface of martensite laths, block boundary and prior austenite grain boundary. Due to the homogenous



**Figure 3.** SEM micrographs of different heat treatments. (a) P-IDP, 740 °C; (b) IDP, 740 °C; (c) P-IDP, 760 °C; (d) IDP, 760 °C; (e) P-IDP, 780 °C; (f) IDP, 780 °C; (g) P-IDP, 800 °C; (h) IDP, 800 °C; (i) P-IDP, 820 °C; (j) IDP, 820 °C.

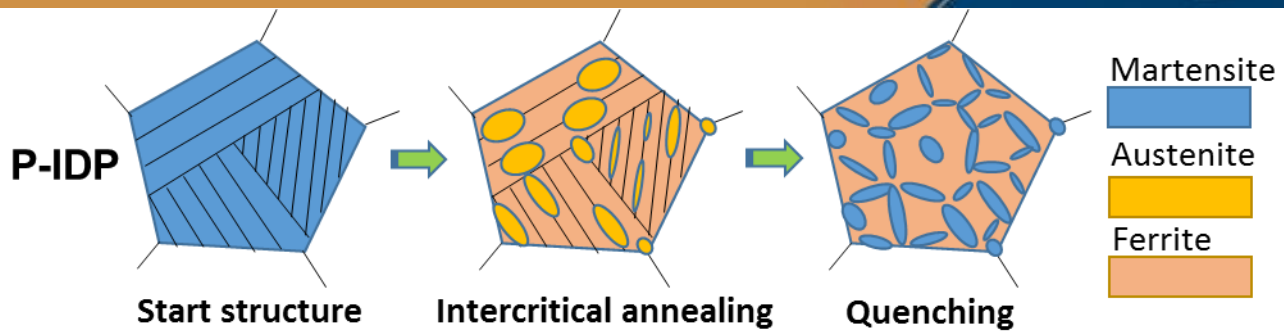


**Figure 4.** Schematic illustration of microstructure evolution of P-IDP.

nucleation with relatively high number density, the initial austenite during annealing or final martensite was much smaller than that of IDP samples, which was comparable to the results of Mazaheri et al [20]. As a result, the banded structure was entirely eliminated in P-IDP samples. This process can be illustrated by the schematic diagram of Fig. 4.

### 3.2 Microstructural characterization by EPMA , EBSD and TEM

Furthermore, as shown in Fig. 5, the carbon and manganese elements are significant enriched in martensite, irrespective of heat treatment. However, the element distributions in P-IDP sample are relatively more homogeneous than that of IDP sample. In order to compare the homogenization of grain size in different heat treatment, the detailed crystallographic analysis of typical IDP and P-IDP samples were conducted by EBSD and the results are shown in Fig. 6. Here, the green lines represent low-angle grain boundaries (LAGBs) with misorientation angles of  $2^{\circ}$ ~ $10^{\circ}$ , while blue lines indicate high-angle grain boundaries (HAGBs) with misorientation angles larger than  $10^{\circ}$ . Based on the EBSD maps of samples suffered from identical annealing process, the grain size that indicated by the HAGBs shows much more homogeneous, while

some ultra-coarse grain with size  $\sim 10\mu\text{m}$  was observed in IDP sample. Meanwhile, it can be found that abundant LAGBs existed in the interior of coarse grain in IDP sample, which is usually determined as unrecrystallized grain with sub-structure [21]. Actually, these results are consistent with the results mentioned in Fig.4.

In reality, the micro-alloyed elements in this paper also play vital role in the microstructure evolution and final mechanical properties. On one hand, the micro-alloyed elements can effectively refine the prior austenite and hence refine the subsequent constituent phases due to large number density of nucleation sites. On the other hand, the micro-alloyed carbides can improve strength by precipitation strengthening effect [22]. Due to the nanoscale of micro-alloyed carbides, the typical P-IDP sample annealed at  $800^{\circ}\text{C}$  was applied to observe nanoscale microstructure by TEM, as shown in Fig. 7. It is obvious that a large number of micro-alloyed carbides precipitated inside ferrite matrix (Fig. 7b), which can be further determined as VC by EDX. The VC can effectively pinned dislocations inside ferrite (Fig. 7a), which can significantly improve the resistance of dislocation glide, and hence improved the macro yield stress.

Moreover, some martensite island was confirmed to be twin martensite with high carbon content, which was ascribed to the carbon enrichment from ferrite into prior

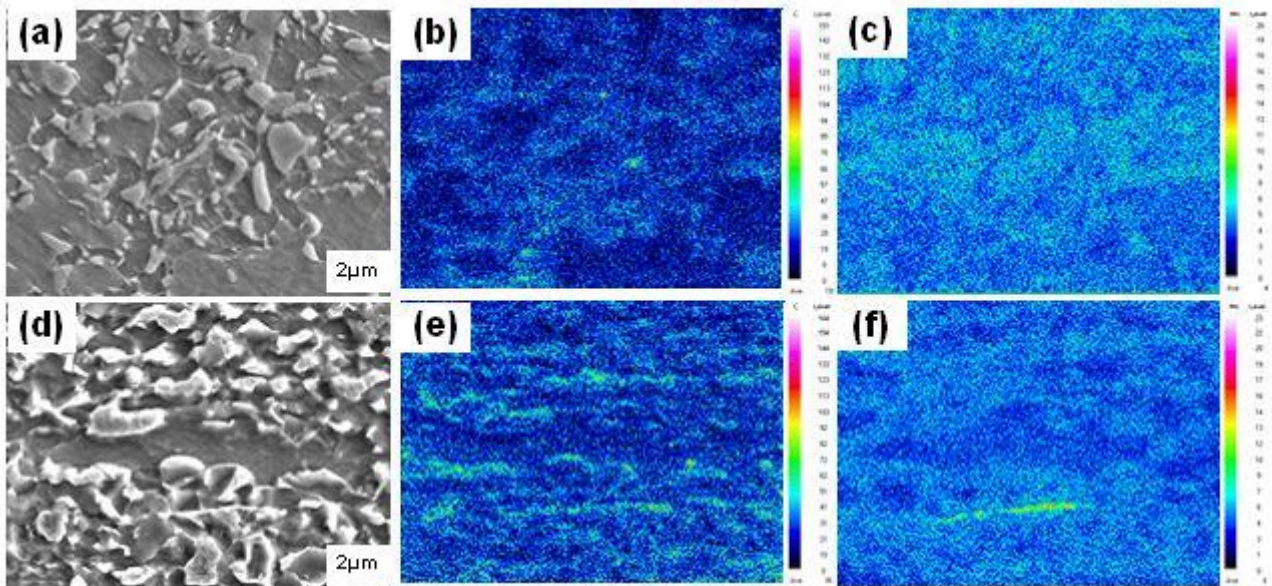


**Figure 5** EPMA results of typical specimens. (a), (b), and (c) correspond to SE image of P-IDP 800 °C, C distribution and Mn distribution, respectively. (d), (e), (f) correspond to SE image of IDP 800 °C, C distribution and Mn distribution, respectively.

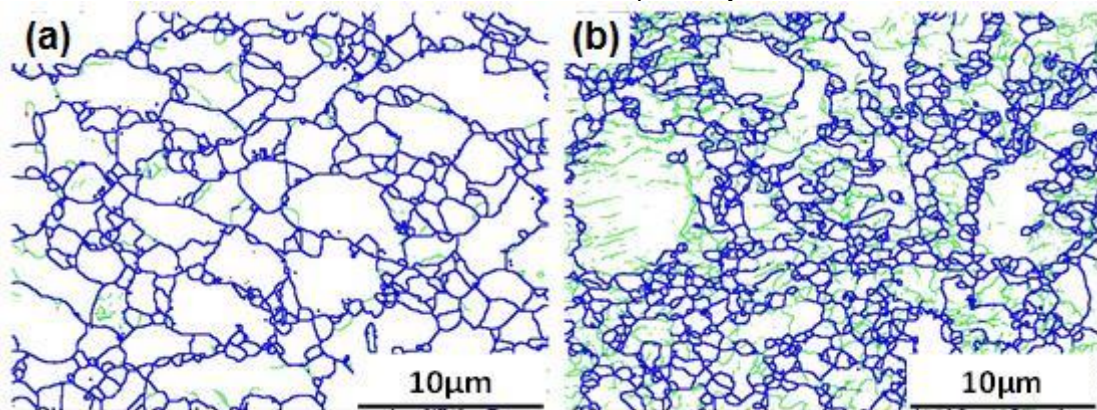


**Figure 6.** Grain boundary distribution of P-IDP and IDP sample annealed at 800 °C for 300s. (a) P-IDP sample; (b) IDP sample. Blue line: high angle grain boundary (>10°), green line: low angle grain boundary (>2°).

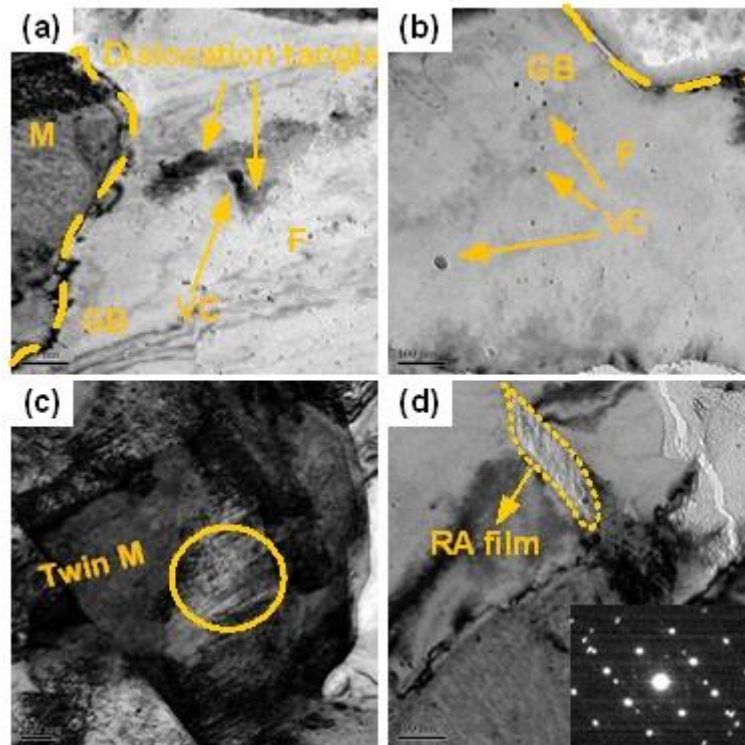


**Figure 7.** TEM images of P-IDP specimen at 800 °C. (a) dislocation pinned by VC (b) VC precipitated inside ferrite matrix; (c) twin martensite and (d) film-like RA. Inserted image indicates diffraction pattern of RA.

austenite during intercritical annealing. In addition, it should be noted that some film-like retained austenite (RA) was also observed, which can be transformed into martensite during deformation to improve the final strength and ductility. This result is also called as transformation induced plasticity (TRIP) effect [23].

### 3.3 Mechanical properties of IDP and P-IDP process

The engineering stress-strain curves of different heat treatments are plotted in Fig. 8. And the corresponding mechanical properties are presented in Fig. 9. Fig. 8(a) clearly shows that the values of ultimate tensile strength and total elongation of the P-IDP samples are much higher than those of IDP samples with identical intercritical annealing parameters. In addition, all of the IDP samples curves exhibited continuous

yielding behavior, typically seen in DP steel. However, as for P-IDP treatments, the samples annealed at 740°C and 760°C exhibited obvious yield platform, which lengths are both approximately 6%. With the increase in annealing temperature, the yield platform entirely disappeared above 780°C. Actually, the occurrence of yield platform can be attributed to the existence of abundant cementite at 740°C and 760°C (Fig. 3a and 3c), which can pinned the dislocation until the stress increased to critical value to conquer the resistance of pinned effect. The length of yield platform is usually related to the heterogeneous deformation of tensile sample.

As shown in Fig. 9, It is clear that the variation trends of YS and UTS in both heat treatments are identical. The largest UTS of IDP treatment was obtained as 1062MPa, when intercritical annealed at



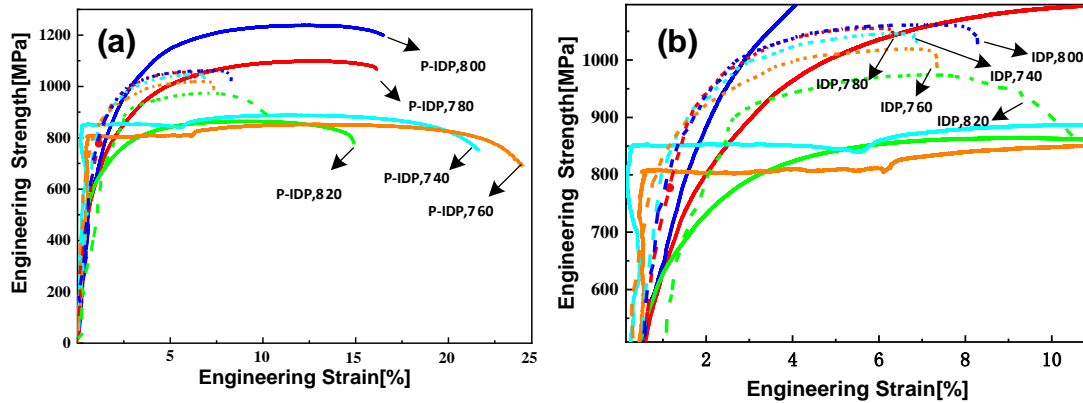


**Figure 8.** (a) Engineering stress-strain curves of IDP and P-IDP samples; (b) enlarged view of curves in (a). Dotted lines correspond to IDP samples, while solid lines represent P-IDP samples

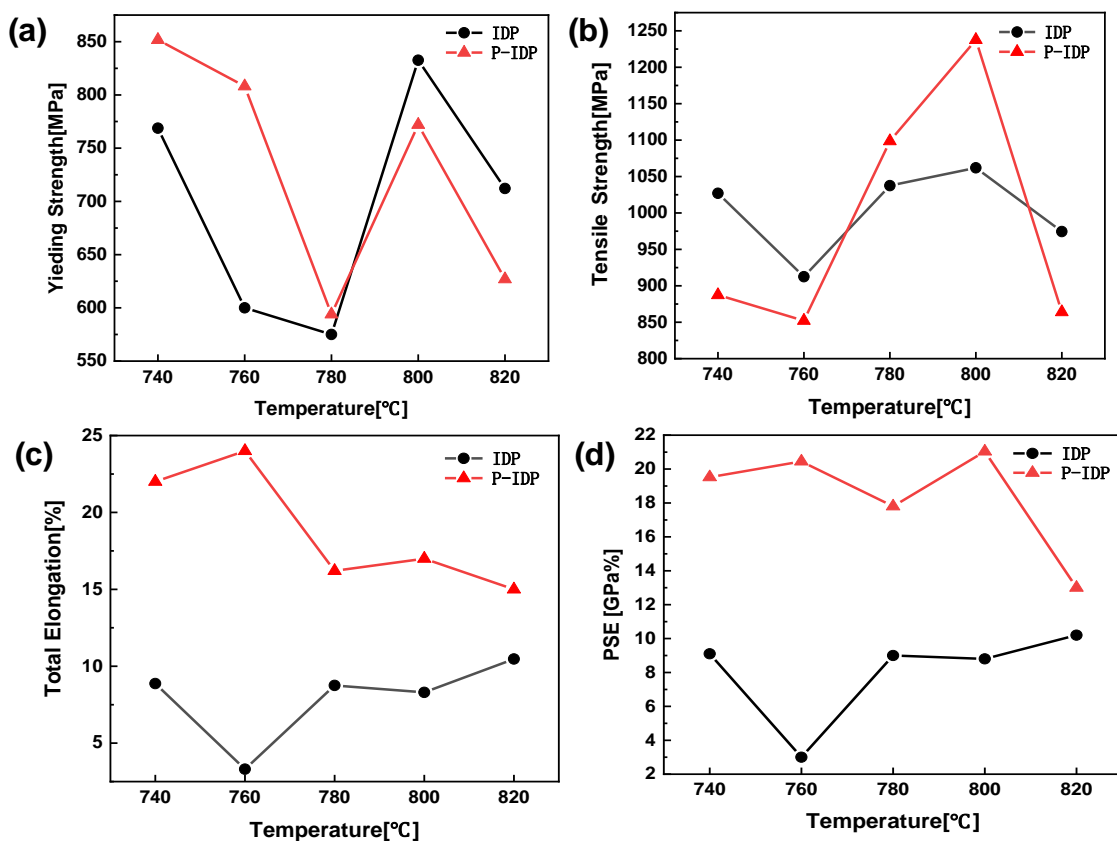


**Figure 9.** Mechanical properties of the samples after IDP and P-IDP treatment : (a) Yielding strength; (b) Ultimate tensile strength; (c) Total elongation; (d) Product of strength and elongation

800°C for 300s, while the maximum UTS of P-IDP samples with identical annealing condition is 1238MPa. Meanwhile, the optimum total elongation (TEL) of P-IDP can reach 24%, while that of IDP samples is 10.5%. It is clear that a better combination of strength and ductility can be obtained in P-IDP samples. Compare the product of strength and elongation (PSE) of two heat treatments, the PSE of

P-IDP sample is about twice larger than that of IDP. The optimal mechanical properties were obtained in P-IDP sample that annealed at 800°C for 300s, in which the maximum PSE exceeding 21GPa% with UTS of 1238MPa and TE of 17%, attributing to the grain refinement, precipitation strengthening effect, homogeneous phase distribution and optimized constituent phase fractions.

## 4 CONCLUSION

A novel heat treatment involving pre-quenching process was applied to obtain microstructure comprising ferrite and martensite. Meanwhile, the corresponding microstructure evolution and mechanical properties were compared with those of traditional intercritical DP steel. The conclusions obtained are as follows:

(1) The microstructure obtained by pre-quenching DP treatment was relatively more refined with homogeneous distribution, whilst ultrafine ferrite grains and chain-networked martensite grains along ferrite grain boundaries were obtained.

(2) The banded structure was significantly observed after conventional DP treatment, while entirely eliminated after the novel pre-quenching DP treatment.

(3) The optimal mechanical properties were obtained by pre-quenching DP treatment, in which the maximum PSE exceeding 21GPa% with UTS of 1238MPa and TE of 17%, attributing to the grain refinement, precipitation strengthening effect, homogeneous phase distribution and optimized constituent phase fractions.

### Acknowledgments

This work was supported by the National Natural Science Foundation of China (Nos.51674080, 51404155 and U1260204), and National Key R&D Program of China (2017YFB0304105).

### REFERENCES

- 1 Jiang ZH, Guan ZZ, Lian JS. Effects of microstructural variables on the deformation behaviour of dual-phase steel. *Mater. Des.* 1995;190:55-64.
- 2 Davies RG. Influence of martensite composition and content on the properties of dual phase steels. *Metallurgical Transactions A.* 1978;9(5):671-679.
- 3 Bouaziz O, Zurob H, Huang MX. Driving force and logic of development of advanced high strength steels for automotive applications. *Steel Res. Int.* 2013;84(10):937-947.
- 4 Chowdhury SG, Pereloma EV, Santos DB. Evolution of texture at the initial stages of continuous annealing of cold rolled dual-phase steel: effect of heating rate. *Materials Science and Engineering: A.* 2008;480(1-2):540-548.
- 5 Cai XH, Liu CB, Liu ZY. Process design and prediction of mechanical properties of dual phase steels with prepositional ultra fast cooling. *Mater. Des.* 2014;53:55-64.
- 6 Calcagnotto M, Ponge D, Raabe D. Effect of grain refinement to 1  $\mu\text{m}$  on strength and toughness of dual-phase steels. *Materials Science and Engineering: A.* 2010;527(29-30):7832-7840.
- 7 Schemmann L, Zaeferrer S, Raabe D, Friedel F, Mattissen D. Alloying effects on microstructure formation of dual phase steels. *Acta Mater.* 2015;95:386-398.
- 8 Ashrafi H, Shamanian M, Emadi R, Saeidi N. A novel and simple technique for development of dual phase steels with excellent ductility. *Materials Science and Engineering: A.* 2017;680:197-202.
- 9 Rosenberg G, Sinaiová I, Juhar L. Effect of microstructure on mechanical properties of dual phase steels in the presence of stress concentrators. *Materials Science and Engineering: A* 2013;582:347-358.
- 10 Song RJ, Fonstein N, Jun HJ, Pottore N, Bhattacharya D, Jansto S. Effects of Nb on Microstructural Evolution and Mechanical Properties of Low-Carbon Cold-Rolled Dual-Phase Steels. *Metallography, Microstructure, and Analysis.* 2014;3(3):174-184.
- 11 Chen CY, Yen HW, Kao FH, Li WC, Huang CY, Yang JR, et al. Precipitation hardening of high-strength low-alloy steels by nanometer-sized carbides. *Materials Science and Engineering: A.* 2009;499(1-2):162-166.
- 12 Hong SC, Lee KS. Influence of deformation induced ferrite transformation on grain refinement of dual phase steel. *Materials Science and Engineering: A.* 2002;323(1-2):148-159.
- 13 M. PapaRao, SubramanyaSarma V, Sankaran S. Development of high strength and ductile ultrafine grained dual

- phase steel with nanosized carbide precipitates in a V-Nb microalloyed steel. *Materials Science and Engineering: A*. 2013;568:171–175.
- 14 Hashemi SG, Eghbali B. Evolution of high strength and ductile ultrafine grained dual phase super ferrite low carbon V-Nb-Mo steel. *Materials Science and Engineering: A*. 2017;705:32-41.
- 15 Calcagnotto M, Adachi Y, Ponge D, Raabe D. Deformation and fracture mechanisms in fine- and ultrafine-grained ferrite/martensite dual-phase steels and the effect of aging. *Acta Mater*. 2011;59(2): 658-670.
- 16 Sun JJ, Jiang T, Wang YJ, Guo SW, Liu YN. Ultrafine grained dual-phase martensite/ferrite steel strengthened and toughened by lamella structure. 2018;734:311-317.
- 17 Cai XL. Garratt-Reed AJ. Owen WS. The development of some dual-phase steel structures from different starting microstructures. *Metallurgical Transactions A*. 1985;16(4):543-557.
- 18 Yang DZ, Brown EL, Matlock DK. Krauss G. Ferrite recrystallization and austenite formation in cold-rolled intercritically annealed steel. *Metallurgical Transactions A*. 1985;16(8):1385–1392.
- 19 Nobuo N, Yusuke A., et al., Dual phase structure formed by partial reversion of cold-deformed martensite. *Materials Science & Engineering A*. 2012;553(9):128–133.
- 20 Mazaheri Y., Kermanpur A, Najafzadeh A, Ghatei Kalashami A. Kinetics of ferrite recrystallization and austenite formation during intercritical annealing of the cold-rolled ferrite/martensite duplex structures. *Metallurgical and Materials Transactions A*. 2016;47(3):1040–1051.
- 21 Shi J, Hu J, Wang C, Wang CY, Dong H, Cao WQ. Ultrafine Grained Duplex Structure Developed by ART-annealing in Cold Rolled Medium-Mn Steels. *Journal of Iron and Steel Research, International*. 2014;21(2):208-214.
- 22 Lee WB. Hong SG. Park GC. Kim KH, Park SH. Influence of Mo on precipitation hardening in hot rolled HSLA steels containing Nb. *Scripta Materialia*. 2000;43(4):319-324.
- 23 De Cooman B.C. Structure–properties relationship in TRIP steels containing carbide-free bainite. *Current Opinion in Solid State and Materials Science*. 2004;8(3–4):285-303.